AIAA JOURNAL
Vol. 36, No. 6, June 1998

Method for Correlating Discharge Coefficients of Film-Cooling Holes

Michael Gritsch,* Achmed Schulz,† and Sigmar Wittig‡
University of Karlsruhe, Karlsruhe 76128, Germany

A method for correlating the discharge coefficient of a 30-deg inclined, cylindrical film-cooling hole over a broad range of engine-like conditions is presented. The flow conditions considered are the pressure ratio across the hole (up to 2.25), the crossflow Mach number at the hole entry side (up to 0.6), and the crossflow Mach number at the hole exit side (up to 1.2). The effects of baseline hole flow as well as hole entry and exit crossflows on discharge coefficient were correlated independently of each other. Therefore, the discharge coefficient of any combination of pressure ratio, external Mach number, and internal Mach number flow case can be predicted. A comparison of predicted and measured discharge coefficients reveals the capability of the method proposed.

Nomenclature

b	= channel width
C_D	= discharge coefficient
D	= film-cooling hole diameter
h	= channel height
I	= momentum flux ratio
L	= film-cooling hole length
Ma	= Mach number
$\dot{m}$	= mass flow rate through film-cooling hole
p	= static pressure
p_t	= total pressure
R	= gas constant
Re_D	= Reynolds number based on film-cooling hole diameter
T_t	= total temperature
Tu	= turbulence intensity
u	= velocity
α	= angle of hole inclination
κ	= ratio of specific heats
ρ	= density

Subscripts

c	= internal flow conditions
extCr	= with crossflow at hole exit
$h,1$	= hole entry conditions
$h,2$	= hole exit conditions
intCr	= with crossflow at hole entry
m	= external flow conditions
noCr	= no crossflow at hole entry and exit

Introduction

TURBINE inlet temperatures of modern gas turbines are far beyond the allowable metal temperatures. Film cooling from discrete holes, usually combined with internal convective cooling, is an efficient method to protect the surface of turbine airfoils from the hot gas flow and keep the blade temperatures at acceptable levels (Fig. 1). Because the film-cooling effectiveness strongly depends on the ejected flow rate, the designer needs to know the discharge coefficient of the film-cooling holes at any operating point of the gas turbine to prevent not only underfeeding but also overfeeding of the holes. Underfeeding leads to reduced cooling effectiveness and, therefore, blade areas with high thermal loads, whereas overfeeding results in an inefficient use of turbine working fluid.

Received Aug. 5, 1997; revision received Dec. 22, 1997; accepted for publication Jan. 27, 1998.

*Dipl.-Ingenieur, Institut für Thermische Strömungsmaschinen, Kaiserstr. 12.
†Dr.-Ingenieur, Institut für Thermische Strömungsmaschinen, Kaiserstr. 12.
‡Professor, Institut für Thermische Strömungsmaschinen, Kaiserstr. 12.

The discharge coefficient, however, depends on many geometrical and aerodynamic parameters, such as hole geometry, pressure ratio, and external and internal crossflows. Discharge coefficients of various film-cooling hole geometries have been studied in the past, e.g., normal cylindrical holes,[1,2] inclined cylindrical holes,[3,4] or shaped holes.[5,6] In some of these reports the effect of internal and external crossflow on the discharge coefficient is discussed. In most cases, however, only a very limited range of crossflow Mach numbers is considered. A comprehensive review of published data on discharge coefficients for gas turbine applications was given recently.[7]

The major objective of the present paper is to derive an empirical approach for predicting discharge coefficients of a film-cooling hole with crossflow on both the entry and exit sides of the hole. For the flow through the hole with crossflow on both sides, pressure losses occur at the hole entry, inside the hole, and at the hole exit. These pressure losses are taken into account independently of each other following a suggestion in the literature.[8,9] However, additional losses due to crossflows are expressed in a relative increase/decrease of the discharge coefficient as compared with the baseline discharge coefficient rather than in terms of additional loss coefficients.

Experimental Apparatus

The present investigation was carried out in a continuous flow wind tunnel at the Institut für Thermische Strömungsmaschinen, Karlsruhe, Germany. Details of the experimental facility were given in an earlier paper.[10] The film-cooling test rig consists of a primary loop representing the external flow and a secondary loop representing the internal flow of an airfoil (Fig. 2). The air for both loops is provided by a high-pressure, high-temperature test facility. However, pressure and flow rate in both loops can be set independently of each other.

Primary Loop

The air supplied passes a metering orifice and flow straighteners before it enters the test section through a Laval nozzle (Fig. 3). The test section is 90 mm in width and 41 mm in height. For supersonic flow conditions, the height is reduced to 32 mm. Using an adjustable upper wall, a zero pressure gradient in the streamwise direction is set in the test section.

Preliminary tests were performed to evaluate the effect of the coolant-to-mainflow-temperature ratio on the discharge coefficient. The tests comprised coolant-to-mainflow-temperature ratios from 0.54 to 1.0. For a fixed pressure ratio, no measurable effect of temperature ratio on discharge coefficient was found as long as the external Mach number was matched. Therefore, the reported measurements were conducted with a mainflow temperature being equal to the coolant flow temperature of about 290 K.

Secondary Loop

The flow in the secondary loop is driven by an additional blower. Thus, the internal crossflow Mach number can be set by adjusting

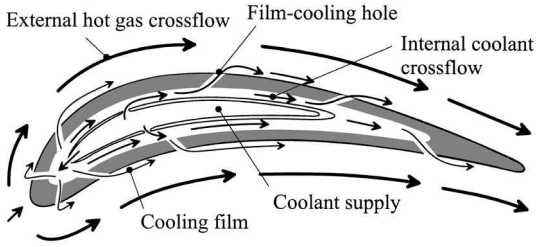

Fig. 1 Flow configuration inside and around a film-cooled nozzle guide vane.

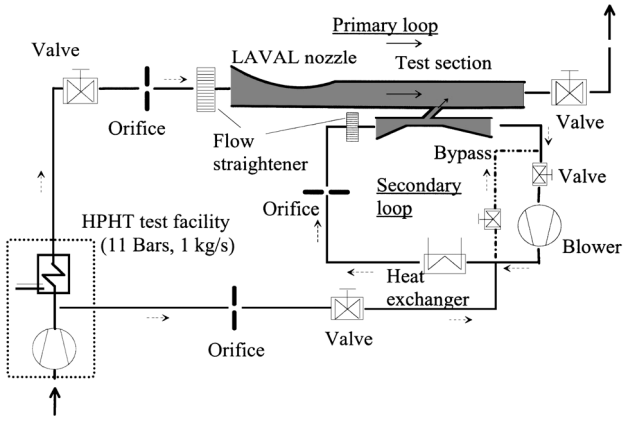

Fig. 2 Film-cooling test rig.

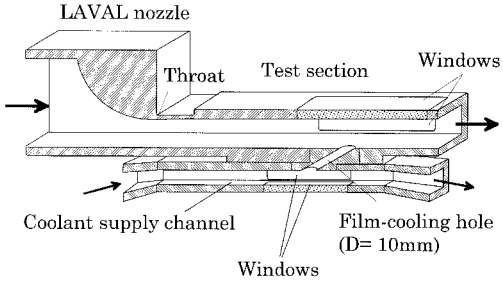

Fig. 3 Film-cooling test section.

the volume flow rate circulating in the secondary loop. The cross-sectional area at the film-cooling hole location is 60 mm in width and 20 mm in height. Because of the closed-loop design of the secondary loop, the flow rate through the film-cooling hole is obtained directly by measuring the flow rate entering the loop, independently of the crossflow rate. Therefore, very accurate measurements of the flow rate through the film-cooling hole, which are imperative for an exact determination of the discharge coefficient, were achieved.[10] For all tests presented in this paper, the primary and secondary loops were oriented parallel to each other, representing a flow condition that occurs, for example, in the midportion of nozzle guide vanes (Fig. 1).

Definition of Discharge Coefficient

The discharge coefficient C_D is the ratio of actual mass flow rate to ideal mass flow rate through the film-cooling hole. The ideal mass flow rate is calculated assuming an isentropic one-dimensional expansion from the total pressure in the secondary loop p_{tc} to the static pressure in the primary loop p_m. This leads to

$$C_D = \dot{m} \Bigg/ \left\{ p_{tc}\left(\frac{p_m}{p_{tc}}\right)^{(\kappa+1)/2\kappa}\left(\frac{\pi}{4}\right)D^2 \times \sqrt{\frac{2\kappa}{(\kappa-1)RT_{tc}}\left[\left(\frac{p_{tc}}{p_m}\right)^{(\kappa-1)/k}-1\right]}\right\} \quad (1)$$

The total pressure and temperature in the coolant channel were measured one hole diameter upstream of the cooling hole inlet with a probe located two hole diameters off the channel centerline. The static pressure in the primary loop was measured at the top wall opposite to the cooling hole exit.

Experimental Program

For the flow through the hole with crossflows, pressure losses occur inside the hole due to wall friction and, more dominant, the forming of a vena contracta. Furthermore, the jet–crossflow interaction at the entry and the exit of the hole can induce additional pressure losses but also gains.

To determine the contribution of the different pressure loss mechanisms, three test cases were considered: 1) no crossflow on both sides of the hole to measure the baseline discharge coefficient of the hole, 2) crossflow on the entry side, and 3) crossflow on the exit side to investigate the additional effect of crossflow on the discharge coefficient. For the present investigation, a single scaled-up cylindrical film-cooling hole ($D = 10$ mm) was drilled in a flat aluminum test plate at an inclination angle of $\alpha = 30$ deg. The length-to-diameter ratio L/D of the hole was 6. Hole entry and exit were sharp edged. The internal surfaces were aerodynamically smooth. The hole was tested for a matrix of pressure ratios ($p_{tc}/p_m = 1, \ldots, 2.25$) and crossflow Mach numbers ($Ma_m = 0.0, \ldots, 1.2$ and $Ma_c = 0.0, \ldots, 0.6$) covering the whole range of engine operating conditions. The complete set of operating conditions is given in Table 1.

Estimates of Accuracy

The uncertainty[11] in the values of the discharge coefficient resulted from the uncertainty in measuring the actual flow rate through the film-cooling hole and the uncertainty in determining the ideal flow rate. Because the secondary loop was designed as a closed loop, the actual flow rate could be measured for all flow cases directly using a standard orifice, leading to a maximum uncertainty of 2.5% except for very low mass flow rates. The uncertainty in determining the ideal flow rate was calculated to be much less than 2% except for very low pressure ratios. Overall, the uncertainty in the values of C_D was found to be less than 2% in most of the cases considered, increasing up to 4.5% for very low pressure ratios and mass flow rates.

Results

No-Crossflow Case

For zero external and internal crossflow, a weak dependence of the discharge coefficient C_D on the pressure ratio p_{tc}/p_m was found (Fig. 4; $Ma_m = 0.0$). There is a slight increase in the discharge coefficient C_D of about 10% when the pressure ratio p_{tc}/p_m is raised from 1 to 2. This effect does not occur for incompressible flows.[12] It is believed to be due to a pressure ratio effect on the cross-sectional area of the vena contracta formed at the hole inlet and was reported before by others.[4,13]

Crossflow at Hole Exit

To evaluate the additional losses due to crossflow at the hole exit, two sets of data were acquired (Figs. 4 and 5). They revealed that the additional losses strongly depend on the pressure ratio as well as the external crossflow Mach number. The crossflow at the exit side of the hole tends to impede the jet exiting from the hole, resulting in lower discharge coefficients compared with the no-crossflow case at the same pressure ratio. The effect is more pronounced at high crossflow Mach numbers and low pressure ratios.

Table 1 Operating conditions of film-cooling test rig

Condition	Value
Internal pressure p_{tc}, bar	<2
Internal temperature T_{tc}, K	290
Pressure ratio p_{tc}/p_m	1, . . . , 2.25
Temperature ratio T_{tc}/T_{tm}	1
Internal Mach number Ma_c	0, . . . , 0.6
External Mach number Ma_m	0, . . . , 1.2
Internal Reynolds number Re_{Dc}	$<2.5 \times 10^5$
External Reynolds number Re_{Dm}	$<2.1 \times 10^5$
Internal turbulence intensity Tu_c, %	1
External turbulence intensity Tu_m, %	<1.5

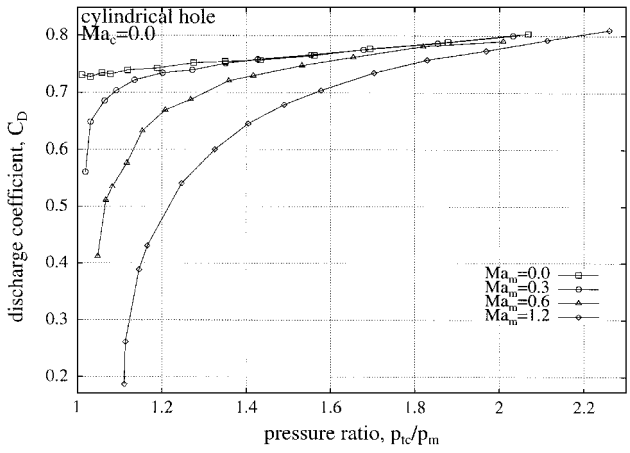

Fig. 4 Discharge coefficient plotted vs pressure ratio with external crossflow applied.

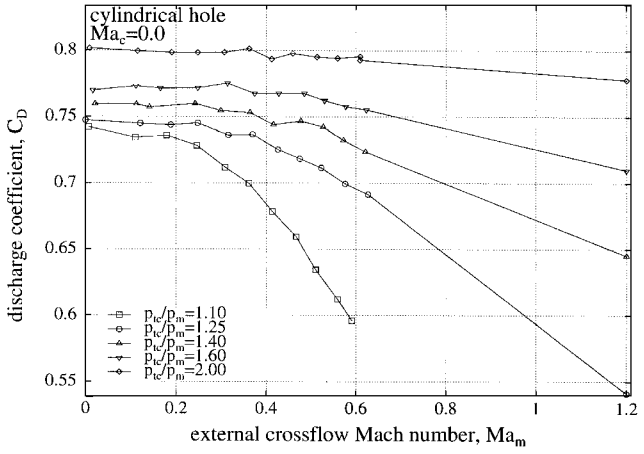

Fig. 5 Discharge coefficient plotted vs external crossflow Mach number.

The results of the discharge coefficient measurements were plotted vs the jet-to-external-crossfbw momentum flux ratio, defined as

$$I_{\text{jet/extCr}} = \frac{(\rho u^2)_{h,2}}{(\rho u^2)_m} \tag{2}$$

which is equal to

$$I_{\text{jet/extCr}} = \frac{(\kappa p Ma^2)_{h,2}}{(\kappa p Ma^2)_m} \tag{3}$$

with

$$Ma_{h,2} = \frac{\dot{m}}{(\pi/4)D^2 p_{h,2}} \sqrt{\frac{RT_{h,2}}{\kappa}} \tag{4}$$

For the case $Ma_m = 0$, $I_{\text{jet/extCr}}$ is not defined according to Eq. (3). Therefore, a fixed value of

$$I_{\text{jet/extCr}} = \left[\frac{(bh)_m}{(\pi/4)D^2}\right]^2 \tag{5}$$

is used to represent the momentum flux ratio for this case (Fig. 6; $Ma_m = 0.0$).

Figure 6 shows that there is a common trend but some scatter in the plot. This is obviously due to the fact that the measured discharge coefficients for the external crossflow case also include the contribution of the baseline pressure losses inside the hole. Therefore, the discharge coefficient was normalized using the discharge coefficient of the no-crossflow case at the same pressure ratio. The normalized discharge coefficient is plotted vs the jet-to-external-crossfbw momentum flux ratio (Fig. 7). It was found that all data collapse to a single curve. At low momentum flux ratios the discharge coefficient is lower than for the no-crossflow case, indicating additional losses due to the external crossflow. If the momentum flux ratio exceeds 2, the effect of crossflow on the discharge coefficient can be neglected.

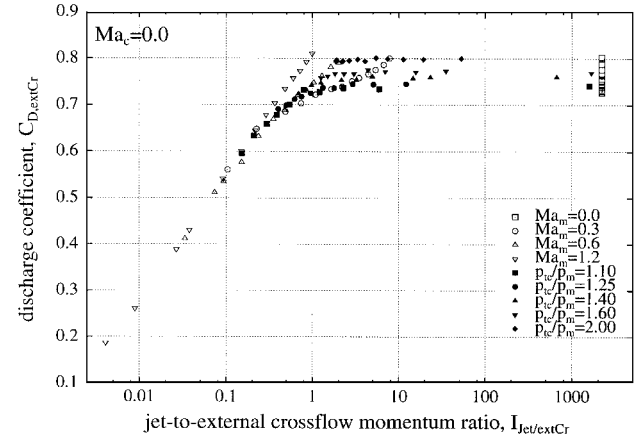

Fig. 6 Discharge coefficient plotted vs jet-to-external-crossflow momentum flux ratio: hole exit side crossflow.

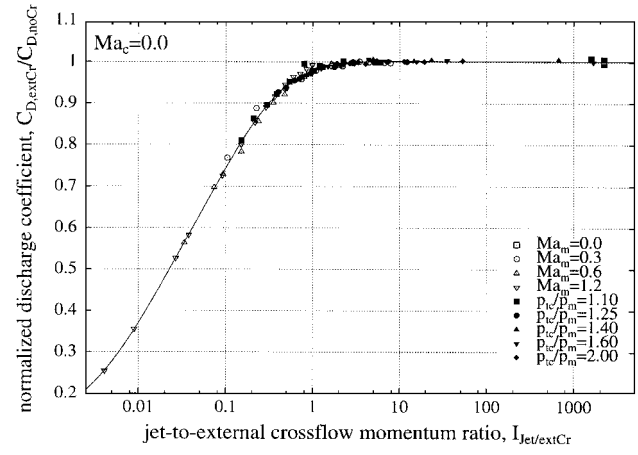

Fig. 7 Normalized discharge coefficient plotted vs jet-to-external-crossflow momentum flux ratio: hole exit side crossflow.

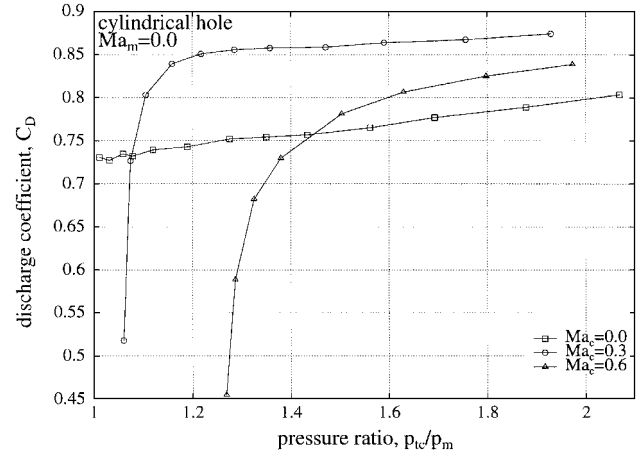

Fig. 8 Discharge coefficient plotted vs pressure ratio with internal crossflow applied.

Crossflow at Hole Entry

The same procedure as for the external crossflow case was applied to evaluate the additional losses due to internal crossflow. However, the effect of internal crossflow is somewhat different from the effect of external crossflow. Figure 8 reveals that the discharge coefficient with internal crossflow can exceed the baseline discharge coefficient without internal crossflow, particularly at elevated pressure ratios. Figure 9 shows that for each pressure ratio an internal crossflow Mach number exists for which the discharge coefficient C_D is at an optimum. The lower the pressure ratio is, the lower is this internal crossflow Mach number $Ma_{c,\text{opt}}$. However, the level of optimum discharge coefficient is almost unaffected by the pressure ratio.

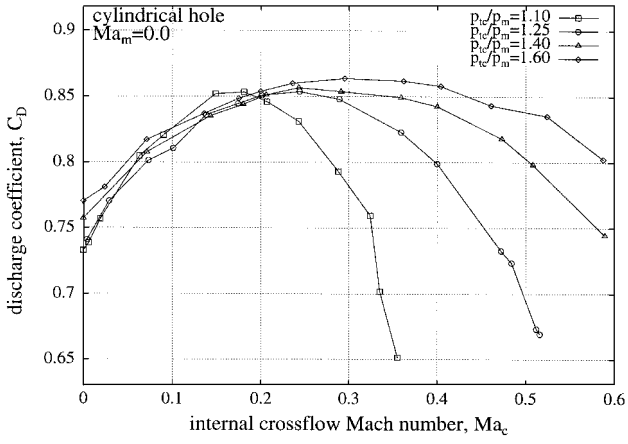

Fig. 9 Discharge coefficient plotted vs internal crossflow Mach number.

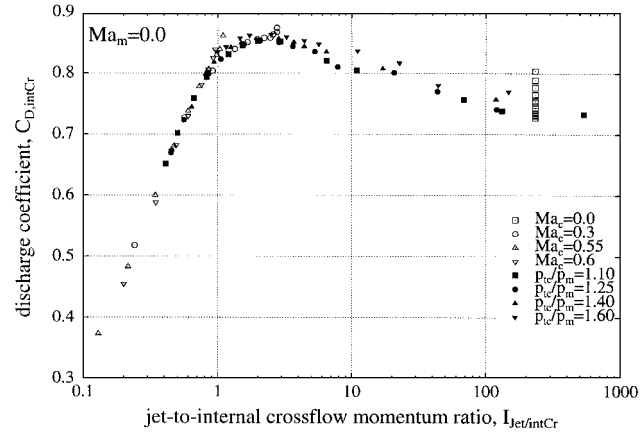

Fig. 10 Discharge coefficient plotted vs jet-to-internal-crossflow momentum flux ratio: hole entry side crossflow.

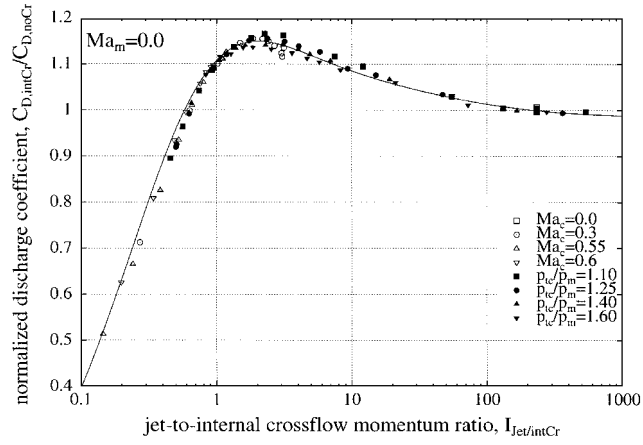

Fig. 11 Normalized discharge coefficient plotted vs jet-to-internal-crossflow momentum flux ratio: hole entry side crossflow.

Flowfield measurements performed inside the cooling hole by means of a laser Doppler velocimetry system showed that the size and location of the separation region at the hole entry are dominated by the internal crossflow Mach number.[14] With no internal crossflow applied ($Ma_c = 0.0$), a separation region was found at the downstream edge of the hole inlet, whereas at high internal crossflow Mach numbers ($Ma_c = 0.5$) a separation region was found at the upstream edge of the hole inlet. For a medium Mach number $Ma_c = 0.3$, most of the jet was found in the center of the hole, indicating that the effect of the separation region is very small, if there is a separation region at all. These findings were confirmed by the present discharge coefficient measurements. The peak value of the discharge coefficient occurs at a crossflow Mach number $Ma_{c,\mathrm{opt}}$ for which the flow enters the hole without jet separation taking place. If the crossflow Mach number is lower than $Ma_{c,\mathrm{opt}}$, separation occurs at the downstream edge of the hole inlet; if the crossflow Mach number is higher than $Ma_{c,\mathrm{opt}}$, separation occurs at the upstream edge of the hole inlet, both producing additional losses and, therefore, resulting in decreased discharge coefficients.

The results of the discharge coefficient measurements were plotted vs the jet-to-internal-crossflow momentum flux ratio, defined as

$$I_{\mathrm{jet/intCr}} = \frac{(\rho u^2)_{h,1}}{(\rho u^2)_c} \tag{6}$$

which is equal to

$$I_{\mathrm{jet/intCr}} = \frac{(\kappa p M a^2)_{h,1}}{(\kappa p M a^2)_c} \tag{7}$$

with

$$Ma_{h,1} = \frac{\dot{m}}{(\pi/4) D^2 p_{h,1}} \sqrt{\frac{R T_{h,1}}{\kappa}} \tag{8}$$

For the $Ma_c = 0.0$ case, $I_{\mathrm{jet/intCr}}$ is not defined according to Eq. (7). Therefore, a fixed value of

$$I_{\mathrm{jet/intCr}} = \left[\frac{(bh)_c}{(\pi/4) D^2} \right]^2 \tag{9}$$

is used to represent the momentum flux ratio for this case (Fig. 10; $Ma_c = 0.0$).

Figure 10 shows that there is a common trend but again some scatter. Using the same scheme as for the exit side crossflow case, the ratio of the discharge coefficient with entry side crossflow to the discharge coefficient without crossflow is plotted vs the jet-to-entry-side crossflow momentum ratio. Figure 11 shows the additional effect of crossflow at the hole entry side. It was found that for momentum flux ratios beyond 0.6 the normalized discharge coefficient exceeds unity. This indicates that the crossflow actually makes it easier for the flow to enter the hole. The maximum of 1.15 occurs at a momentum flux ratio of 2. At very large momentum flux ratios, however, no additional effect of the entry side crossflow was found. It becomes obvious that the arbitrary definitions of the momentum flux ratios for the case of zero crossflow [Eqs. (5) and (9)] do not hamper the data collapsing to a single curve because the normalized discharge coefficients are not affected by the momentum flux ratio for $I_{\mathrm{jet/extCr}} > 2$ and $I_{\mathrm{jet/intCr}} > 100$.

Prediction and Validation

The measured discharge coefficients of the two crossflow cases were correlated by least-square curvefits represented by the solid lines in Figs. 7 and 11. Because it is now possible to account for the effects of baseline hole flow, hole entry crossflow, and hole exit crossflow separately, the discharge coefficient of any flow case can be predicted using the following calculation procedure:

$$C_D(p_{tc}/p_m, I_{\mathrm{jet/intCr}}, I_{\mathrm{jet/extCr}}) = C_{D\mathrm{noCr}}(p_{tc}/p_m) \times C_{D\mathrm{intCr}}/C_{D\mathrm{noCr}}(I_{\mathrm{jet/intCr}}) \times C_{D\mathrm{extCr}}/C_{D\mathrm{noCr}}(I_{\mathrm{jet/extCr}}) \tag{10}$$

Because the momentum flux of the hole flow itself depends on the overall discharge coefficient, an iterative calculation of the discharge coefficient is necessary, e.g., by means of a small computer program. Total pressures, total temperatures, and crossflow Mach numbers at hole entry and exit have to be entered to describe the flow configuration.

To validate the proposed method, additional discharge coefficient measurements with crossflow on both sides were performed. Two test cases were chosen. First, the hole exit crossflow Mach number was kept constant ($Ma_m = 0.6$) while the hole entry crossflow Mach number Ma_c was varied from 0.0 to 0.6. Second, the hole entry crossflow Mach number was kept constant ($Ma_c = 0.6$) while the hole exit crossflow Mach number Ma_m was varied from 0.0 to 1.2. Figures 12 and 13 show a comparison of the measured and predicted discharge coefficients. The excellent agreement between measured and predicted values clearly demonstrates the capability of the proposed method.

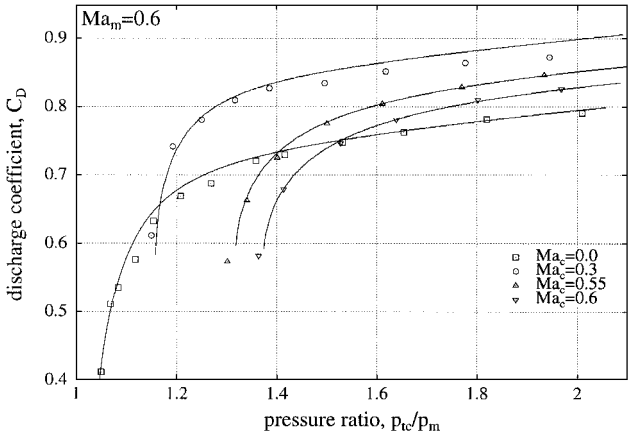

Fig. 12 Comparison of measured and predicted discharge coefficients; Ma_m = 0.6.

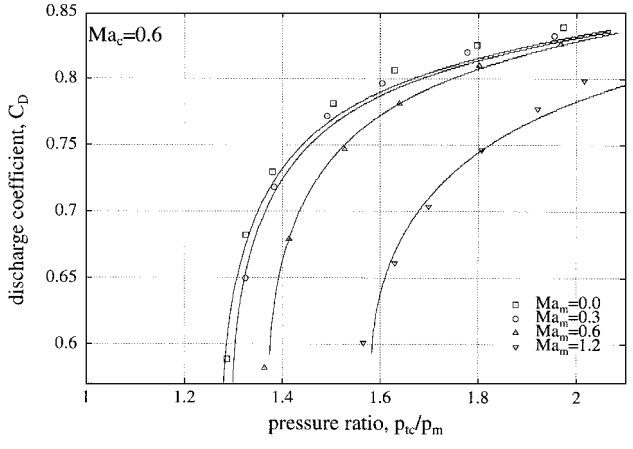

Fig. 13 Comparison of measured and predicted discharge coefficients; Ma_c = 0.6.

The empirical correlations of the present paper are, of course, limited to the specific geometry of the film-cooling hole and the orientation of the internal crossflow channel. The intention of the paper was to develop a method of correlating the discharge coefficient rather than to present a complete set of correlations for different hole geometries. However, the method was also applied to other hole geometries tested in the course of the present research program, such as cylindrical holes with a different inclination angle or with an additional rotation angle (compound angle holes). It was found that for these holes predictions also showed good agreement with measured data. Because the proposed method is based on the assumption that the hole entry flow does not affect the hole exit flow and the losses can be predicted independently of each other, the agreement was found to be the better the longer the hole was. The authors strongly believe that the method can be easily transferred to other hole geometries such as holes with rounded entries and exits. Future work of the authors will particularly address the application of the presented method to flow configurations where the internal crossflow is directed not parallel but perpendicular to the external crossflow.

Conclusions

A method for correlating the discharge coefficient of a 30-deg inclined, cylindrical film-cooling hole was presented. The method was based on the assumption that the losses inside the hole as well as at the hole's entry and exit can be predicted independently of each other. The losses inside the hole were found to depend on the pressure ratio across the hole, whereas the additional losses at the hole's entry and exit depend on the hole jet-to-crossflow momentum flux ratio. Using these correlations, the overall discharge coefficient of any flow configuration can be predicted. A comparison of predicted and measured discharge coefficients showed excellent agreement and demonstrated the capability of the method proposed.

Acknowledgment

This study was partly funded by the European Union through a grant by the Brite Euram program, "Investigation of the Aerodynamics and Cooling of Advanced Engine Turbine Components," under Contract AER2-CT92-0044.

References

[1] Hay, N., Lampard, D., and Benmansour, S., "Effect of Crossflows on the Discharge Coefficient of Film Cooling Holes," *Journal of Engineering for Power*, Vol. 105, No. 2, 1983, pp. 243–248.

[2] Tillman, E. S., Hartel, E. O., and Jen, H. F., "The Prediction of Flow Through Leading Edge Holes in a Film Cooled Airfoil with and Without Inserts," American Society of Mechanical Engineers, ASME Paper 84-GT-4, New York, June 1984.

[3] Hay, N., Henshall, S. E., and Manning, A., "Discharge Coefficients of Holes Angled to the Flow Direction," *Journal of Turbomachinery*, Vol. 116, No. 1, 1994, pp. 92–96.

[4] Hay, N., Lampard, D., and Khaldi, A., "The Coefficient of Discharge of 30° Inclined Film Cooling Holes with Rounded Entries or Exits," American Society of Mechanical Engineers, ASME Paper 94-GT-180, New York, June 1994.

[5] Hay, N., and Lampard, D., "The Discharge Coefficient of Flared Film Cooling Holes," American Society of Mechanical Engineers, ASME Paper 95-GT-15, New York, June 1995.

[6] Gritsch, M., Schulz, A., and Wittig, S., "Discharge Coefficient Measurements of Film-Cooling Holes with Expanded Exits," American Society of Mechanical Engineers, ASME Paper 97-GT-165, New York, June 1997.

[7] Hay, N., and Lampard, D., "Discharge Coefficient of Turbine Cooling Holes: A Review," American Society of Mechanical Engineers, ASME Paper 96-GT-492, New York, June 1996.

[8] Sasaki, M., Takahara, K., Sakata, K., and Kumagai, T., "Study on Film Cooling of Turbine Blades," *Bulletin of the Japan Society of Mechanical Engineers*, Vol. 19, Nov. 1976, pp. 1344–1352.

[9] Tillman, E. S., and Jen, H. F., "Cooling Airflow Studies at the Leading Edge of a Film-Cooled Airfoil," *Journal of Engineering for Gas Turbines and Power*, Vol. 106, No. 1, 1984, pp. 214–221.

[10] Wittig, S., Schulz, A., Gritsch, M., and Thole, K. A., "Transonic Film-Cooling Investigations: Effects of Hole Shapes and Orientations," American Society of Mechanical Engineers, ASME Paper 96-GT-222, New York, June 1996.

[11] Kline, S. J., and McClintock, F. A., "Describing Uncertainties in Single-Sample Experiments," *Mechanical Engineering*, Vol. 75, Jan. 1953, pp. 3–8.

[12] Lichtarowicz, A., Duggins, R. K., and Markland, E., "Discharge Coefficients for Incompressible Non-Cavitating Flow Through Long Orifices," *Journal of Mechanical Engineering Science*, Vol. 7, No. 2, 1965, pp. 210–219.

[13] Jackson, R. A., "The Compressible Discharge of Air Through Small Thick Plate Orifices," *Applied Scientific Research*, Vol. A13, 1963, pp. 241–248.

[14] Thole, K. A., Gritsch, M., Schulz, A., and Wittig, S., "Effect of a Crossflow at the Entrance to a Film-Cooling Hole," *Journal of Fluids Engineering*, Vol. 119, No. 3, 1997, pp. 533–541.

A. Plotkin
Associate Editor